

Measurement of Br photofragment orientation and alignment from HBr photodissociation: Production of highly spin-polarized hydrogen atoms

T. Peter Rakitzis, P. C. Samartzis, R. L. Toomes, and Theofanis N. Kitsopoulos

Citation: *The Journal of Chemical Physics* **121**, 7222 (2004); doi: 10.1063/1.1794691

View online: <http://dx.doi.org/10.1063/1.1794691>

View Table of Contents: <http://scitation.aip.org/content/aip/journal/jcp/121/15?ver=pdfcov>

Published by the [AIP Publishing](#)

Articles you may be interested in

[Spin-polarized hydrogen Rydberg time-of-flight: Experimental measurement of the velocity-dependent H atom spin-polarization](#)

Rev. Sci. Instrum. **85**, 053103 (2014); 10.1063/1.4871995

[Laser detection of spin-polarized hydrogen from HCl and HBr photodissociation: Comparison of H- and halogen-atom polarizations](#)

J. Chem. Phys. **129**, 144302 (2008); 10.1063/1.2989803

[Photodissociation of H I and D I : Polarization of atomic photofragments](#)

J. Chem. Phys. **122**, 084301 (2005); 10.1063/1.1850465

[Two-photon state selection and angular momentum polarization probed by velocity map imaging: Application to H atom photofragment angular distributions from the photodissociation of two-photon state selected HCl and HBr](#)

J. Chem. Phys. **121**, 11802 (2004); 10.1063/1.1809571

[Measurement of Cl and Br photofragment alignment using slice imaging](#)

J. Chem. Phys. **116**, 9228 (2002); 10.1063/1.1473801



Measurement of Br photofragment orientation and alignment from HBr photodissociation: Production of highly spin-polarized hydrogen atoms

T. Peter Rakitzis

Department of Physics, University of Crete, P.O. 2208, 71003 Voutes-Heraklion, Greece and Institute of Electronic Structure and Laser, Foundation for Research and Technology-Hellas, 711 10 Heraklion-Crete, Greece

P. C. Samartzis

Department of Chemistry, University of Crete, Leof. Knosou, 71409 Heraklion, Greece and Institute of Electronic Structure and Laser, Foundation for Research and Technology-Hellas, 711 10 Heraklion-Crete, Greece

R. L. Toomes

Institute of Electronic Structure and Laser, Foundation for Research and Technology-Hellas, 711 10 Heraklion-Crete, Greece

Theofanis N. Kitsopoulos

Department of Chemistry, University of Crete, Leof. Knosou, 71409 Heraklion, Greece and Institute of Electronic Structure and Laser, Foundation for Research and Technology-Hellas, 711 10 Heraklion-Crete, Greece

(Received 7 July 2004; accepted 27 July 2004)

The orientation and alignment of the $^2P_{3/2}$ and $^2P_{1/2}$ Br photofragments from the photodissociation of HBr is measured at 193 nm in terms of $a_q^{(k)}(p)$ parameters, using slice imaging. The $A^1\Pi$ state is excited almost exclusively, and the measured $a_q^{(k)}(p)$ parameters and the spin-orbit branching ratio show that the dissociation proceeds predominantly via nonadiabatic transitions to the $a^3\Pi$ and $1^3\Sigma^+$ states. Conservation of angular momentum shows that the electrons of the nascent H atom cofragments (recoiling parallel to the photolysis polarization) are highly spin polarized: about 100% for the Br($^2P_{1/2}$) channel, and 86% for the Br($^2P_{3/2}$) channel. A similar analysis is demonstrated for the photodissociation of HCl. © 2004 American Institute of Physics. [DOI: 10.1063/1.1794691]

I. INTRODUCTION

The measurement of photofragment angular momentum polarization, and the spatial decomposition of this polarization into coherent and incoherent contributions from multiple dissociative states, has intensified in recent years since the quantum mechanical treatment of Siebbeles *et al.*¹⁻⁴ These contributions to the photofragment angular distributions can be expressed in terms of the $a_q^{(k)}(p)$ parameters,⁵ where (p) denotes whether the contribution originates (incoherently) from a dissociative transition that is parallel (\parallel) or perpendicular (\perp), or (coherently) from the interference between parallel and perpendicular transitions (\parallel, \perp). The measurement of each $a_q^{(k)}(p)$ parameter gives specific information about the dissociation process. Recently, for hydrogen halide photodissociation, Balint-Kurti *et al.* expressed $a_q^{(k)}(p)$ in terms of adiabatic and nonadiabatic-transfer probabilities, and in terms of phase shifts between asymptotic wave functions of dissociative states.⁶ Therefore, measurement of $a_q^{(k)} \times (p)$ allows the most complete understanding of the dissociation process, and detailed comparison with theory.

Polarized atoms and nuclei are used to study spin-dependent effects in atomic, molecular, nuclear, and surface collisions. The possibility of the production of highly polarized atoms from molecular photodissociation was suggested by van Brunt and Zare.⁷ The measurement of atomic photofragment polarization [such as the measurement of the complete set of $a_q^{(k)}(p)$ parameters] allows the identification of

systems that yield highly polarized fragments. Strongly polarized atomic photofragments have been measured for O,^{8,9} S,¹⁰⁻¹² Cl,¹³⁻¹⁶ Br,^{11,13} and H.¹² The present study investigates the potential of HBr as a source of highly polarized H and Br photofragments.

Recently, the alignment parameters $a_0^{(2)}(\perp)$ and $a_2^{(2)} \times (\perp)$ were measured for Br($^2P_{3/2}$) from the photodissociation of HBr at 193 nm using slice imaging,^{17,18} a variant of ion imaging,¹⁹ and velocity mapping.²⁰ For HCl, it was shown that the H atom cofragments were strongly spin polarized, demonstrating that photodissociation can provide an intense source of spin-polarized hydrogen. The aim of this paper is to determine the Br(2P_J) and H cofragment polarization as well, and to include in the analysis the effects of the polarization parameters $a_q^{(k)}(p)$ with $k \leq 3$ for the Br($^2P_{3/2}$) and Cl($^2P_{3/2}$) photofragments from the photodissociation of HBr and HCl at 193 nm. $a_q^{(k)}(p)$ can then be expressed in terms of dynamically significant variables such as nonadiabatic transition probabilities and asymptotic phase differences.⁶ From these expressions, we deduce the degree of polarization of the photofragments, and the nonadiabatic dissociation mechanisms.

II. THEORY

The spatial distribution of *unpolarized* photofragments about the linearly polarized photolysis direction light is given by the well-known expression.²¹

$$I(\theta) = I_0[1 + \beta P_2(\cos \theta)], \quad (1)$$

where β is the spatial anisotropy parameter, which, for prompt photodissociation of a diatomic molecule, ranges from -1 (for a pure perpendicular transition) to $+2$ (for a pure parallel transition), and I_0 is a constant. However, a more complicated expression is required for the description of the angular distribution of photofragments which have been detected in a fashion sensitive to angular momentum polarization of the fragments [such as resonantly enhanced multiphoton ionization or caser-induced fluorescence]. When the photolysis and probe polarization directions are parallel (for either linearly or circularly polarized light), and for $J \leq 3/2$, the photofragment angular distribution is given by:

$$I(\theta) = I_0[1 + \beta_2 P_2(\cos \theta) + \beta_4 P_4(\cos \theta)], \quad (2)$$

where I_0 , β_2 , and β_4 are parameters that depend on β and $a_q^{(k)}(p)$. The experiments reported in this paper deal with a single laser geometry, that with counterpropagating photolysis and probe lasers, which are both circularly polarized.

For the $\text{Br}(^2P_{1/2})$ and $\text{Cl}(^2P_{1/2})$ photofragments, k is limited to 1 (as $k \leq 2J$). In this case, $\beta_4 = 0$, and I_0 and β_2 expressed in terms of β , $a_0^{(1)}(\perp)$, and $\text{Re}[a_1^{(1)}(\parallel, \perp)]$ by:^{22,23}

$$I_0 = 1 + \frac{s_1}{3} [(1 - \beta/2)a_0^{(1)}(\perp) + \sqrt{2} \text{Re}[a_1^{(1)}(\parallel, \perp)]], \quad (3)$$

$$\beta_2 = \frac{1}{I_0} \left[\frac{2s_1}{3} \left((1 - \beta/2)a_0^{(1)}(\perp) - \frac{\sqrt{2}}{2} \text{Re}[a_1^{(1)}(\parallel, \perp)] \right) - \beta/2 \right], \quad (4)$$

where s_1 is the experimental sensitivity to the $k=1$ parameters, which depends on the details of the detection transition (given in the Experimental section). The value of β for both $\text{Br}(^2P_{1/2})$ and $\text{Cl}(^2P_{1/2})$ has been measured previously, therefore there are only two unknowns, $a_0^{(1)}(\perp)$ and $\text{Re}[a_1^{(1)}(\parallel, \perp)]$. It is convenient to measure I_0 only as a relative quantity, such as the ratio of I_0 between the two polarization geometries $I_0[RL]/I_0[RR]$ (where the first R indicates that the photolysis polarization is circularly polarized, and the second R or L indicates that the probe polarization is either right or left circularly polarized, respectively). This ratio is given by the ratio of Eq. (3), measured for the two geometries. Another equation can be generated by subtracted the β_2 values for these two geometries: $\Delta\beta_2 = \beta_2(RL) - \beta_2(RR)$, using Eq. (4). These two equations can be solved for the two unknowns $a_0^{(1)}(\perp)$ and $\text{Re}[a_1^{(1)}(\parallel, \perp)]$ in terms of the experimental observables $I_0[RL]/I_0[RR]$ and $\Delta\beta_2$.

For the $\text{Br}(^2P_{3/2})$ and $\text{Cl}(^2P_{3/2})$ photofragments, k is limited to 3, and now I_0 , β_2 , and β_4 are expressed in terms of $k=2$ and $k=3$ parameters as well. The complete inversion of all the $a_q^{(k)}(p)$ with $k \leq 3$ would require more detection geometries or detection transitions (beyond the one used here). However, in this particular case, the contribution of several parameters are negligible, so that approximations can be made to reduce the number of unknown parameters to be equal to the set of experimental observables.

The contributions from the $k=2$ and $k=3$ parameters will be significantly less than the $k=1$ parameters, mainly because these parameters are reduced more by hyperfine depolarization (the $k=1, 2$, and 3 parameters are reduced by factors of 0.5, 0.27, and 0.2, respectively). Therefore, for a first approximation, the data for the ($^2P_{3/2}$) photofragments can be analyzed with the $k=1$ parameters only, using Eqs. (3) and (4), as for the ($^2P_{1/2}$) photofragments. It will be interesting to compare this analysis to a more complete analysis including higher order $a_q^{(k)}(p)$ parameters.

We can express the ($^2P_{3/2}$) photofragment angular distributions in terms of the non-negligible (in this case) $k=2$ and $k=3$ $a_q^{(k)}(p)$ parameters:

$$I_0 = 1 + \frac{s_1}{3} [(1 - \beta/2)a_0^{(1)}(\perp) + \sqrt{2} \text{Re}[a_1^{(1)}(\parallel, \perp)]] + \frac{(1 - \beta/2)s_2}{15} [a_0^{(2)}(\perp) - 2\sqrt{6}a_2^{(2)}(\perp)], \quad (5)$$

$$\beta_2 = \frac{1}{I_0} \left[\frac{2s_1}{3} \left((1 - \beta/2)a_0^{(1)}(\perp) - \frac{\sqrt{2}}{2} \text{Re}[a_1^{(1)}(\parallel, \perp)] \right) + \frac{4(1 - \beta/2)s_2}{21} (4a_0^{(2)}(\perp) + \sqrt{6}a_2^{(2)}(\perp)) + \frac{s_3}{7} \left(3(1 - \beta/2)a_0^{(3)}(\perp) - \frac{8\sqrt{3}}{2} \text{Re}[a_1^{(3)}(\parallel, \perp)] \right) - \beta/2 \right], \quad (6)$$

$$\beta_4 = \frac{1}{I_0} \left\{ \frac{(1 - \beta/2)s_2}{35} (6a_0^{(2)}(\perp) - 2\sqrt{6}a_2^{(2)}(\perp)) + \frac{4s_3}{7} [(1 - \beta/2)a_0^{(3)}(\perp) + \sqrt{3} \text{Re}[a_1^{(3)}(\parallel, \perp)]] \right\}. \quad (7)$$

The parameters $a_0^{(2)}(\parallel)$ and $a_2^{(3)}(\perp)$ have been omitted from Eqs. (5)–(7) because their contribution to the experimental signals (for the experiments considered in this paper) can be neglected. The contribution of the $a_0^{(2)}(\parallel)$ parameter is weighted by $(1 + \beta)$; for both Cl and $\text{Br}(^2P_{3/2})$ photofragments, $\beta = -1$, so that $(1 + \beta) \approx 0$ [the magnitude of the contribution of $a_0^{(2)}(\parallel)$ parameter is a few times smaller than the sensitivity of the experiment] and therefore $a_0^{(2)}(\parallel)$ can be neglected. The $a_2^{(3)}(\perp)$ parameter is proportional to $\sin \Delta\varphi_{Aa}$,⁶ where $\Delta\varphi_{Aa}$ is the asymptotic phase shift between the $A^1\Pi$ state and $a^3\Pi$ state ($\Omega=0$ component). The phase shift was both measured¹¹ and predicted²⁴ to be approximately zero at this photodissociation wavelength; therefore, the contribution from the $a_2^{(3)}(\perp)$ parameter can also be neglected in this case. Furthermore, both $a_0^{(1)}(\perp)$ and $a_0^{(3)}(\perp)$ can be expressed in terms of nonadiabatic transition probabilities between the $A^1\Pi$ and $a^3\Pi$ states (see the Discussion section); these expressions allow, in this case, $a_0^{(3)}(\perp)$ to be related in terms of $a_0^{(1)}(\perp)$:

$$a_0^{(3)}(\perp) = \left[\frac{4}{5} a_0^{(1)}(\perp) - \frac{2}{\sqrt{15}} \right]. \quad (8)$$

Using these approximations, we have reduced the number of unknown parameters to 3 the $a_0^{(1)}(\perp)$, $\text{Re}[a_1^{(1)}(\parallel, \perp)]$, and $\text{Re}[a_1^{(3)}(\parallel, \perp)]$. As with Eqs. (3) and (4) for the ($^2P_{1/2}$) atoms, Eqs. (5)–(7) can be used to generate three new equations: $I_0[RL]/I_0[RR]$, $\Delta\beta_2$, and $\Delta\beta_4$. These three equations can be solved for the three unknowns.

III. EXPERIMENT

The apparatus has been described in detail elsewhere.^{14,25} Briefly, a 10 Hz pulsed molecular beam containing 5% HBr or HCl in He is skimmed and collimated, and is intersected at right angles by two counter propagating laser beams. The photolysis laser beam is generated by an ArF excimer laser (COMPEX, Lambda Physik); the linearly polarized Brewster reflection from a suprasil window is then circularly polarized with a quarter-wave plate, and is focused onto the molecular beam ($f=25$ cm). The probe laser beam is generated by MOPO-SL (Spectra Physics 730DT10), and is also made circularly polarized using a quarter-wave plate. The $\text{Br}(^2P_{3/2})$ and $\text{Br}(^2P_{1/2})$ photofragments are ionized using the two-photon resonant transitions $5p(^2P_{1/2}) \leftarrow 4p^5(^2P_{3/2})$ at 250.41 nm and $5p(^2P_{3/2}) \leftarrow 4p^5(^2P_{1/2})$ at 263.12 nm, whereas the $\text{Cl}(^2P_{3/2})$ and $\text{Cl}(^2P_{1/2})$ photofragments are ionized at $4p(^2P_{1/2}) \leftarrow 3p^5(^2P_{3/2})$ at 234.62 nm and $4p(^2P_{3/2}) \leftarrow 3p^5(^2P_{1/2})$ at 236.51 nm, respectively.^{26–28} For the ionization of the $^2P_{3/2}$ photofragments, for right (upper sign) and left (lower sign) circularly polarized light, the s_k are given by: $s_1 = \mp 3\sqrt{3/5}(1/2)$, $s_2 = +(5/4)(10/37)$, and $s_3 = \mp \sqrt{15/4}(1/5)$ (note that the long-time-limit hyperfine depolarization coefficients are included in these factors; $1/2$ for $k=1$, $10/37$ for $k=2$, and $1/5$ for $k=3$).²⁹ For the $^2P_{1/2}$ atoms, $s_1 = \mp \sqrt{3}(1/2)$ (which includes the depolarization coefficient of $1/2$). Using the slice-imaging technique, 400 ns after the photofragment ionization, the extraction field is pulsed ON, and the Br^+ or Cl^+ ions are accelerated towards the ion-imaging detector. Ions of different mass separate in their time-of-flight during their field-free trajectory on route to the detector. The detector gain is pulsed ON for ~ 20 ns at the proper arrival time for slice-imaging velocity selection.¹⁴ Images appearing on the detector anode are recorded using a charged-coupled device camera (Cohu 4910, using EYESPY Software by k -Space Associates Inc.). Images are taken without Doppler scanning. Effects of Doppler selection are removed by normalizing the images with images taken with both photolysis and probe polarizations linear and perpendicular to the imaging plane.¹³

IV. RESULTS

The $\text{Br}(^2P_{3/2})$ and $\text{Br}(^2P_{1/2})$ photofragment slice images are shown for the RR and RL polarization geometries in Fig. 1. The angular distributions (also shown in Fig. 1) are determined by integrating the signal within the full width at half maximum of the Br-photofragment slice-image radius as a function of θ . The angular distributions are normalized with the corresponding ZZ angular distribution (for which both

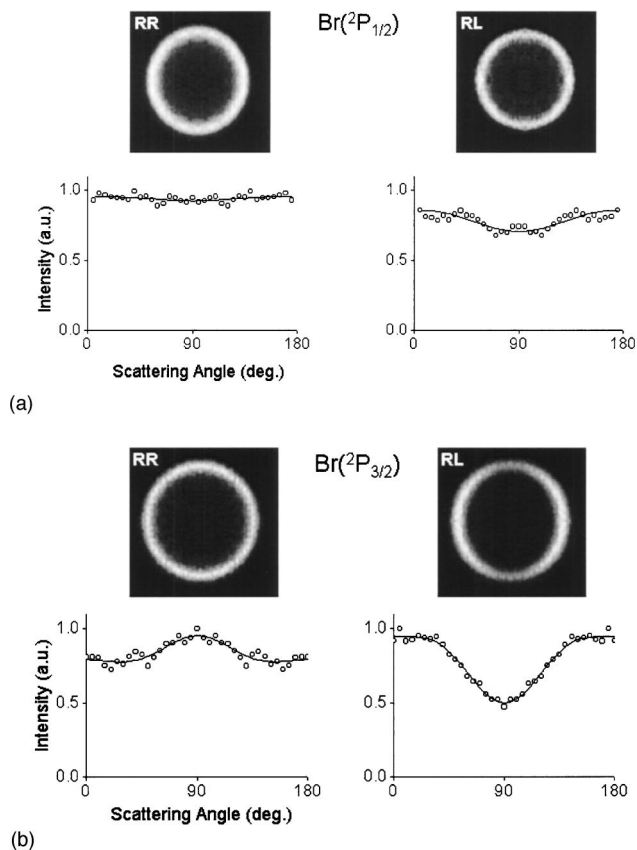


FIG. 1. (a) $\text{Br}(^2P_{1/2})$ and $\text{Br}(^2P_{3/2})$ photofragments slice images following the photolysis of HBr at 193 nm. The photolysis laser is right (R) circularly polarized, and the counterpropagating probe laser is right (R) or left (L) circularly polarized. These distinct polarization geometries are denoted RR and RL , respectively. (b) The $\text{Br}(^2P_{1/2})$ and $\text{Br}(^2P_{3/2})$ photofragment angular distributions calculated from the images shown in (a) (and described in the text).

the photolysis and probe are linearly polarized parallel to the time-of-flight axis) and are then fit to Eq. (2).¹³ The slice images and angular distributions for $\text{Cl}(^2P_{3/2})$ and $\text{Cl}(^2P_{1/2})$ are shown elsewhere.¹² The variations in I_0 , β_2 , and β_4 between the RL and RR geometries are given by $I_0[RL]/I_0[RR]$, $\Delta\beta_2$, and $\Delta\beta_4$ are shown in Table I for both $\text{B}(^2P_J)$ and $\text{Cl}(^2P_J)$.

The polarization of the $\text{Br}(^2P_{1/2})$ photofragments is described by the $a_0^{(1)}(\perp)$ and $\text{Re}[a_1^{(1)}(\parallel, \perp)]$ parameters only (because $k \leq 2J$, and is limited to 1 in this case). The values for the variations in intensity and angular distributions [given by $I_0[RL]/I_0[RR]$ and $\Delta\beta_2$ described in the Theory and Re-

TABLE I. The Br and $\text{Cl}(^2P_J)$ difference anisotropy parameters, $\Delta\beta_2 = \beta_2(RL) - \beta_2(RR)$, and $\Delta\beta_4 = \beta_4(RL) - \beta_4(RR)$, and the intensity ratios $I_0[RL]/I_0[RR]$ [see Eqs. (1) and (2)]. The first R indicates that the photolysis polarization is right circularly polarized, and the second R or L indicates that the probe polarization is either right or left circularly polarized, respectively. For the $\Delta\beta_2$ and $\Delta\beta_4$, $\sigma=0.05$, and for $I_0[RL]/I_0[RR]$, $\sigma=0.1$.

	$\text{Br}(^2P_{3/2})$	$\text{Br}(^2P_{1/2})$	$\text{Cl}(^2P_{3/2})$	$\text{Cl}(^2P_{1/2})$
$\Delta\beta_2$	0.63	0.20	0.97	0.33
$\Delta\beta_4$	-0.23	-0.03	-0.11	0.02
$I_0[RL]/I_0[RR]$	1.6	1.75	1.4	1.8

TABLE II. Calculated polarization parameters for Br and Cl(2P_J), using the experimental data from Table I and Eqs. (3)–(7). Measurements of β , $a_0^{(2)}(\perp)$, and $a_2^{(2)}(\perp)$ are given from Ref. 11. Error bars are 2σ .

	Br($^2P_{3/2}$)	Br($^2P_{1/2}$)	Cl($^2P_{3/2}$)	Cl($^2P_{1/2}$)
β	-0.88 ± 0.10	-0.21 ± 0.10	-0.97 ± 0.06	-0.87 ± 0.06
$a_0^{(1)}(\perp)$	$+0.30 \pm 0.07$	$+0.55 \pm 0.16$	$+0.39 \pm 0.08$	$+0.60 \pm 0.10$
$\text{Re}[a_1^{(1)}(\parallel, \perp)]$	$+0.09 \pm 0.08$	$+0.46 \pm 0.16$	-0.06 ± 0.10	$+0.32 \pm 0.12$
$a_0^{(2)}(\perp)$	-0.7 ± 0.2	...	-0.5 ± 0.2	...
$a_2^{(2)}(\perp)$	-0.3 ± 0.2	...	-0.45 ± 0.2	...
$\text{Re}[a_1^{(3)}(\parallel, \perp)]$	-0.22 ± 0.14	...	-0.12 ± 0.15	...

sults sections, determined from fitting with Eq. (1) and given in Table I, are inserted into Eqs. (3) and (4). These two equations are then solved for $a_0^{(1)}(\perp)$ and $\text{Re}[a_1^{(1)}(\parallel, \perp)]$ parameters, shown in Table II and Fig. 2. Note that even though $\Delta\beta_2$ for the Br($^2P_{1/2}$) photofragments is small, the values of the $a_0^{(1)}(\perp)$ and $\text{Re}[a_1^{(1)}(\parallel, \perp)]$ parameters are found to be near maximal because of the large value of the $I_0[RL]/I_0[RR]$ ratio. In particular, $a_0^{(1)}(\perp)$ and $\text{Re}[a_1^{(1)}(\parallel, \perp)]$ parameters are both large and positive, so that they largely cancel in Eq. (4) to give a small value of $\Delta\beta_2$, and add in Eq. (3) to give a large value of $I_0[RL]/I_0[RR]$.

For the Br($^2P_{3/2}$) photofragments, the angular momentum distributions can be described by the perpendicular-transition alignment parameters, $a_0^{(1)}(\perp)$, $a_0^{(2)}(\perp)$, and $a_2^{(2)}(\perp)$, as well as the $\text{Re}[a_1^{(1)}(\parallel, \perp)]$ and $\text{Re}[a_1^{(3)}(\parallel, \perp)]$ interference parameters; the contribution from the $a_0^{(2)}(\parallel)$, $\text{Re}[a_1^{(2)}(\parallel, \perp)]$, and $a_2^{(3)}(\perp)$ are neglected as the contributions to the experimental signals are too small to be measured in the current experiments. The values of β , $a_0^{(2)}(\perp)$, and $a_2^{(2)}(\perp)$ used in Eqs. (5)–(7) (and shown in Table II) are from Ref. 11. Right and left circularly polarized probe light are equally sensitive to the β , $a_0^{(2)}(\perp)$, and $a_2^{(2)}(\perp)$ parameters, therefore they do not strongly affect the values of the orientation parameters determined here; in particular, the relatively large error bars of the $a_0^{(2)}(\perp)$ and $a_2^{(2)}(\perp)$ parameters do not strongly affect the error bars of the orientation parameters. The values for the variations in intensity and angular distributions from Eq. (2), given by $I_0[RL]/I_0[RR]$, $\Delta\beta_2$ and

$\Delta\beta_4$, are inserted into Eqs. (5)–(7). These three equations are then solved for $a_0^{(1)}(\perp)$, $\text{Re}[a_1^{(1)}(\parallel, \perp)]$, and $\text{Re}[a_1^{(3)}(\parallel, \perp)]$ parameters, shown in Table II and Fig. 2.

It is worth noting that if the ($^2P_{3/2}$) data is analyzed ignoring the $k=2$ and $k=3$ parameters, using Eqs. (3) and (4), then, for Br($^2P_{3/2}$) $a_0^{(1)}(\perp)=0.38$ and $\text{Re}[a_1^{(1)}(\parallel, \perp)]=0.04$, and for Cl($^2P_{3/2}$) $a_0^{(1)}(\perp)=0.42$ and $\text{Re}[a_1^{(1)}(\parallel, \perp)]=-0.13$. These numbers deviate less than 10% of the physical range of the parameters from the more complete analysis using $k=2$ and $k=3$ parameters as well. Therefore, it seems that the $k=1$ parameters can be measured fairly accurately to a first approximation by ignoring the higher-order parameters in this case. However, this approximation is unlikely to hold in cases where the higher-order parameters are not reduced by hyperfine depolarization, such as in $O(^1D)$ and $S(^1D)$.

V. DISCUSSION

HBr is optically excited at 193 nm predominantly via the perpendicular transition $A^1\Pi \leftarrow X^1\Sigma^+$, and at this photodissociation wavelength the spatial anisotropy β of the Br($^2P_{3/2}$) photofragments is close to the limiting value of -1 .^{11,30–33} Here we use the value of $\beta=-0.88$ we have reported previously,¹¹ which may indicate a small contribution of an $\Omega=0$ component to the excitation of about 4%. In contrast, the $a^3\Pi$ ($\Omega=0$ component) $\leftarrow X^1\Sigma_0^+$ transition to the production of Br($^2P_{1/2}$) photofragments is about 25%. The phase difference between states i and j is denoted by $\Delta\varphi_{i,j}$. In terms of the phase shift between the $a^3\Pi$ ($\Omega=0$ component) state and the $1^3\Sigma_1^+$ state, $a_q^{(k)}(p)$ for the ($^2P_{1/2}$) atoms are given by

$$a_0^{(1)}(\perp) = \frac{1}{\sqrt{3}}, \tag{9}$$

$$\text{Re}[a_1^{(1)}(\parallel, \perp)] = \frac{2}{3\sqrt{3}} \sqrt{(1+\beta)(1-\beta/2)} \cos \Delta\varphi_{a,0,3\Sigma}. \tag{10}$$

We see from Fig. 1(a) that the measured values of the $a_0^{(1)}(\perp)$ and $\text{Re}[a_1^{(1)}(\parallel, \perp)]$ parameters, for the Br($^2P_{1/2}$) photofragments, correspond, approximately, to the maximal physical range of these parameters. Therefore, the measured $a_0^{(1)}(\perp)$ is in agreement with Eq. (9), and the maximal value of $\text{Re}[a_1^{(1)}(\parallel, \perp)]$ implies that $\cos \Delta\varphi_{a,0,3\Sigma}$ is also approximately maximal.

The Ω components of the $A^1\Pi$ and $a^3\Pi$ states that participate in the dissociation, and yield ($^2P_{3/2}$) atoms, correlate asymptotically to the atomic states $|m_A, m_B\rangle$ as

$$|\pm 1\rangle_A \xrightarrow{R \rightarrow \infty} \left| \mp \frac{1}{2}, \pm \frac{3}{2} \right\rangle, \tag{11}$$

$$|\pm 1\rangle_a \xrightarrow{R \rightarrow \infty} \left| \pm \frac{1}{2}, \pm \frac{1}{2} \right\rangle, \tag{12}$$

$$|0\rangle_a \xrightarrow{R \rightarrow \infty} \left| \mp \frac{1}{2}, \pm \frac{1}{2} \right\rangle. \tag{13}$$

For the ($^2P_{3/2}$) atoms $a_q^{(k)}(p)$ are given by

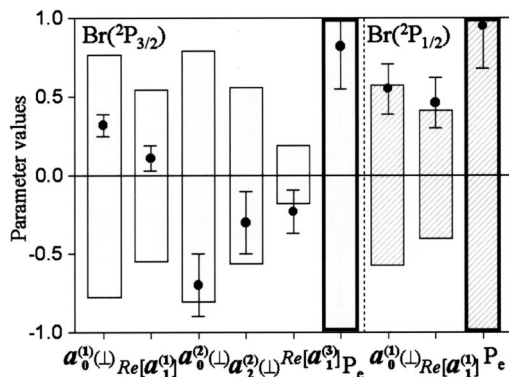


FIG. 2. The measured $a_q^{(k)}(p)$ polarization parameters for the nascent Br($^2P_{1/2}$) and Br($^2P_{3/2}$) photofragments and the inferred nascent H-atom electron polarization P_e from the photodissociation of HBr at 193 nm.

$$a_0^{(1)}(\perp) = + \frac{(3-2p)}{\sqrt{15}}, \quad (14)$$

$$\text{Re}[a_1^{(1)}(\parallel, \perp)] = c_{A,a0} \cos \Delta \varphi_{A,a0} + c_{a1,a0} \cos \Delta \varphi_{a1,a0}, \quad (15)$$

$$a_0^{(2)}(\perp) = +(4/5)(1-2p), \quad (16)$$

$$a_2^{(2)}(\perp) = -(4\sqrt{2}/5)\sqrt{p(1-p)}\cos \Delta \varphi_{A,a1}, \quad (17)$$

$$a_0^{(3)}(\perp) = \frac{2(1-4p)}{5\sqrt{15}}, \quad (18)$$

where p is equal to $p_1/(1-p_2)$; p_1 and p_2 is the probability of nonadiabatic transfer from the $A^1\Pi$ to the $a^3\Pi$ state and $1^3\Sigma_1$ state, respectively. Notice that Eq. (18) differs from Eq. (21) in Ref. (6), due to a different convention.

Using either Eq. (14) or Eq. (16), we can solve for p , and obtain 0.93 ± 0.13 . The probability p_2 was measured to be about $2(0.14)/3$,^{33,34} hence we determine p_1 to be 0.80 ± 0.10 . Therefore, after excitation to the primary absorber, the $A^1\Pi$ state, only 6% dissociates adiabatically [Eq. (11)], whereas 80% transfers nonadiabatically to the $a^3\Pi$ state [Eq. (12)] and 14% to the $1^3\Sigma_1$ state, both of which involve an H spin flip. Using $p=0.93$ and Eq. (17), we see that $\Delta \varphi_{A,a1}=0$. The $\text{Re}[a_1^{(1)}(\parallel, \perp)]$ parameter is small, and therefore we cannot separate the possibility that both the contributions from $\Delta \varphi_{A,a0}$ and $\Delta \varphi_{a1,a0}$ are small [Eq. (15)], or that they are canceling each other.

The populations of the m states of the ($^2P_{3/2}$) photofragments recoiling parallel to the photodissociation polarization direction are given in terms of the $a_q^{(k)}(p)$ by

$$p(J=3/2, m_Z = \pm 3/2) = \frac{1}{4} \left[1 \pm \frac{9}{\sqrt{15}} a_0^{(1)}(\perp) + \frac{5}{4} a_0^{(2)}(\perp) \pm \frac{\sqrt{15}}{2} a_0^{(3)}(\perp) \right], \quad (19)$$

$$p(J=3/2, m_Z = \pm 1/2) = \frac{1}{4} \left[1 \pm \frac{3}{\sqrt{15}} a_0^{(1)}(\perp) - \frac{5}{4} a_0^{(2)}(\perp) \mp \frac{3\sqrt{15}}{2} a_0^{(3)}(\perp) \right]. \quad (20)$$

The electron polarization P_e of the nascent H atoms, also recoiling parallel to the photodissociation polarization direction, is given by the difference in population between the $m=1/2$ and $m=3/2$ states of the halogen ($^2P_{3/2}$) state:

$$P_e = -\frac{1}{4} \left[\frac{6}{\sqrt{15}} a_0^{(1)}(\perp) + \frac{5}{2} a_0^{(2)}(\perp) + 2\sqrt{15} a_0^{(3)}(\perp) \right]. \quad (21)$$

Using Eqs. (8) and (21), and the measured values of $a_0^{(1)}(\perp)$ and $a_0^{(2)}(\perp)$, the nascent electron polarization for the H atoms (parallel to the photodissociation propagation direction) from the photodissociation of HBr is determined

to be $86 \pm 27\%$ (2σ). The theoretical electron polarization for the H atoms corresponding to $\text{Br}(^2P_{1/2})$ atoms is 100%. Therefore, the overall H-atom electron polarization is about 88%. The degree of this polarization may be confirmed both directly³⁵ and theoretically,³⁶ and the polarization may increase at different photodissociation wavelengths.²¹ This work shows that HBr photodissociation can be used as an intense source of spin-polarized hydrogen.

ACKNOWLEDGMENTS

This work is conducted at the Ultraviolet Laser Facility operating at FORTH-IESL (Improving Human Potential-Transnational Access to major Research Infrastructures, Grant No. HPRI-CT-1999-00074) and is also supported by Grant Nos. HPRN-CT-2002-00183 (PICNIC) and HPRN-CT-2000-0006 (REACTIVES).

- ¹L. D. A. Siebbeles, M. Glass-Maujean, O. S. Vasyutinskii, J. A. Beswick, and O. Roncero, *J. Chem. Phys.* **100**, 3610 (1994).
- ²A. S. Bracker, E. R. Wouters, A. G. Suits, Y. T. Lee, and O. S. Vasyutinskii, *Phys. Rev. Lett.* **80**, 1626 (1998).
- ³A. S. Bracker, E. R. Wouters, A. G. Suits, and O. S. Vasyutinskii, *J. Chem. Phys.* **110**, 6749 (1999).
- ⁴T. P. Rakitzis, S. A. Kandel, A. J. Alexander, Z. H. Kim, and R. N. Zare, *J. Chem. Phys.* **110**, 3351 (1999).
- ⁵T. P. Rakitzis and R. N. Zare, *J. Chem. Phys.* **110**, 3341 (1999).
- ⁶G. G. Balint-Kurti, A. J. Orr-Ewing, J. A. Beswick, A. Brown, and O. S. Vasyutinskii, *J. Chem. Phys.* **116**, 10760 (2002).
- ⁷R. J. van Brunt and R. N. Zare, *J. Chem. Phys.* **48**, 4304 (1968).
- ⁸A. T. J. B. Eppink, D. H. Parker, M. H. M. Janssen, B. Buijssse, and W. J. van der Zande, *J. Chem. Phys.* **108**, 1305 (1998).
- ⁹M. Ahmed, D. S. Peterka, A. S. Bracker, O. S. Vasyutinskii, and A. G. Suits, *J. Chem. Phys.* **110**, 4115 (1999).
- ¹⁰Y. Mo, H. Katayanagi, M. C. Heaven, and T. Suzuki, *Phys. Rev. Lett.* **77**, 830 (1996).
- ¹¹T. P. Rakitzis, P. C. Samartzis, and T. N. Kitsopoulos, *Phys. Rev. Lett.* **87**, 123001 (2001).
- ¹²D. Townsend, S. K. Lee, and A. G. Suits, *Chem. Phys.* **301**, 197 (2004).
- ¹³A. S. Bracker, E. R. Wouters, A. G. Suits, and O. S. Vasyutinskii, *J. Chem. Phys.* **110**, 6749 (1999).
- ¹⁴T. P. Rakitzis, P. C. Samartzis, R. L. Toomes, L. Tsigaridas, M. Coriou, D. Chestakov, A. T. J. B. Eppink, D. H. Parker, and T. N. Kitsopoulos, *Chem. Phys. Lett.* **364**, 115 (2002).
- ¹⁵T. P. Rakitzis, P. C. Samartzis, R. L. Toomes, T. N. Kitsopoulos, A. Brown, G. G. Balint-Kurti, O. S. Vasyutinskii, and J. A. Beswick, *Science* **200**, 300 (1936).
- ¹⁶T. P. Rakitzis and T. N. Kitsopoulos, *J. Chem. Phys.* **116**, 9228 (2002).
- ¹⁷C. R. Gebhardt, T. P. Rakitzis, P. C. Samartzis, V. Ladopoulos, and T. N. Kitsopoulos, *Rev. Sci. Instrum.* **72**, 3848 (2001).
- ¹⁸R. L. Toomes, P. C. Samartzis, T. P. Rakitzis, and T. N. Kitsopoulos, *Chem. Phys.* **301**, 209 (2004).
- ¹⁹D. W. Chandler and P. L. Houston, *J. Chem. Phys.* **87**, 1445 (1987).
- ²⁰A. T. J. B. Eppink and D. H. Parker, *Rev. Sci. Instrum.* **68**, 3477 (1997).
- ²¹R. N. Zare, *Mol. Photochem.* **4**, 1 (1972).
- ²²A. J. Alexander, Z. H. Kim, S. A. Kandel, R. N. Zare, T. P. Rakitzis, Y. Asano, and S. Yabushita, *J. Chem. Phys.* **113**, 9022 (2000).
- ²³T. P. Rakitzis, *Chem. Phys. Lett.* **342**, 121 (2001).
- ²⁴A. Brown, G. G. Balint-Kurti, and O. S. Vasyutinskii, *J. Phys. Chem.* (in press).
- ²⁵P. C. Samartzis, I. Sakellariou, T. Gougousi, and T. N. Kitsopoulos, *J. Chem. Phys.* **107**, 43 (1997).
- ²⁶S. Arepalli, N. Presser, D. Robie, and R. J. Gordon, *Chem. Phys. Lett.* **118**, 88 (1985).
- ²⁷C. E. Moore, *Atomic Energy Levels as Derived From the Analyses of Optical Spectra* (U.S. Dept. of Commerce, National Bureau of Standards, Washington, 1949).

- ²⁸NIST Atomic Spectra Database Levels Form, http://physics.nist.gov/cgi-bin/AtData/levels_form
- ²⁹A. J. Orr-Ewing and R. N. Zare, *Annu. Rev. Phys. Chem.* **45**, 315 (1994).
- ³⁰M. J. Cooper, E. Wrede, A. J. Orr-Ewing, and M. N. R. Ashfold, *J. Chem. Soc., Faraday Trans.* **94**, 2901 (1998).
- ³¹Y. Matsumi, K. Tonokura, and M. Kawasaki, *J. Chem. Phys.* **97**, 1065 (1992).
- ³²G. Péoux, M. Monnerville, T. Duboo, and B. Pouilly, *J. Chem. Phys.* **107**, 70 (1997).
- ³³Z. Xu, B. Koplitz, and C. Wittig, *J. Phys. Chem.* **92**, 5518 (1988).
- ³⁴R. Baumfalk, U. Buck, C. Frischkorn, N. H. Nahler, and L. Hüwel, *J. Chem. Phys.* **111**, 2595 (1999).
- ³⁵T. P. Rakitzis, *ChemPhysChem* (in press).
- ³⁶Alex Brown, G. G. Balint-Kurti, and O. S. Vasylutinskii *et al.* (unpublished).